



Homoplasy or plesiomorphy? Reconstruction of the evolutionary history of mitochondrial gene order rearrangements in the subphylum Neodermata

Dong Zhang^{a,b}, Wen X. Li^a, Hong Zou^a, Shan G. Wu^a, Ming Li^a, Ivan Jakovlić^c, Jin Zhang^c, Rong Chen^c, Guitang Wang^{a,*}

^a Key Laboratory of Aquaculture Disease Control, Ministry of Agriculture, and State Key Laboratory of Freshwater Ecology and Biotechnology, Institute of Hydrobiology, Chinese Academy of Sciences, Wuhan 430072, PR China

^b University of Chinese Academy of Sciences, Beijing, PR China

^c Bio-Transduction Lab, Wuhan 430075, PR China

ARTICLE INFO

Article history:

Received 8 February 2019

Received in revised form 15 May 2019

Accepted 22 May 2019

Available online 8 August 2019

Keywords:

Gene rearrangement pathway

Mitochondrial phylogenomics

Plesiomorphic gene order state

Phylogenetic marker

ABSTRACT

Recent mitogenomic studies have exposed a gene order (GO) shared by two classes, four orders and 31 species ('common GO') within the flatworm subphylum Neodermata. There are two possible hypotheses for this phenomenon: convergent evolution (homoplasy) or shared ancestry (plesiomorphy). To test those, we conducted a meta-analysis on all available mitogenomes to infer the evolutionary history of GO in Neodermata. To improve the resolution, we added a newly sequenced mitogenome that exhibited the common GO, *Euryhaliotrema johni* (Ancyrocephalinae), to the dataset. Phylogenetic analyses conducted on two datasets (nucleotides of all 36 genes and amino acid sequences of 12 protein coding genes) and four algorithms (MrBayes, RAxML, IQ-TREE and PhyloBayes) produced topology instability towards the tips, so ancestral GO reconstructions were conducted using TreeREx and MLGO programs using all eight obtained topologies, plus three unique topologies from previous studies. The results consistently supported the second hypothesis, resolving the common GO as a plesiomorphic ancestral GO for Neodermata, Cestoda, Monopisthocotylea, Cestoda + Trematoda and Cestoda + Trematoda + Monopisthocotylea. This allowed us to trace the evolutionary GO scenarios from each common ancestor to its descendants amongst the Monogenea and Cestoda classes, and propose that the common GO was most likely retained throughout all of the common ancestors, leading to the extant species possessing the common GO. Neodermatan phylogeny inferred from GOs was largely incongruent with all 11 topologies described above, but it did support the mitogenomic dataset in resolving Polyopisthocotylea as the earliest neodermatan branch. Although highly derived GOs might be of some use in resolving isolated taxonomic and phylogenetic uncertainties, we conclude that, due to the discontinuous nature of their evolution, they tend to produce artefactual phylogenetic relationships, which makes them unsuitable for phylogenetic reconstruction in Neodermata. Wider and denser sampling of neodermatan mitogenomic sequences will be needed to infer the evolutionary pathways leading to the observed diversity of GOs with confidence.

© 2019 Australian Society for Parasitology. Published by Elsevier Ltd. All rights reserved.

1. Introduction

Metazoan mitochondrial genomes typically contain 36 or 37 genes: 22 tRNAs, two rRNAs, and 12 or 13 protein coding genes (PCGs). Assuming an equal probability of relocation for each gene, the total number of theoretically possible gene orders (GO) is tremendously large: 1.376×10^{43} (37!) or 3.72×10^{41} (36!). As a

consequence, convergence of gene orders is believed to be highly unlikely, so identical GOs are generally believed to be an indicator of shared ancestry (Boore and Brown, 1998). Therefore, GO comparisons can throw light on historical relationships of genome architectures and on the evolutionary history of species (Dobzhansky and Sturtevant, 1938; Littlewood et al., 2006). As reviewed by Boore and Brown (1998), mitochondrial (mt) GO possesses a number of idiosyncrasies that make it a good phylogenetic tool: nearly constant gene content, selective neutrality (although this is debatable), near certainty of gene homology, and unlikely

* Corresponding author.

E-mail address: gtwang@ihb.ac.cn (G. Wang).

GO homoplasy (Boore and Brown, 1998; Boore and Fuerstenberg, 2008; Kilpert et al., 2012). In particular, GOs should evolve in a discontinuous, non-clocklike manner, making them perfectly suitable for complementing molecular sequences which generally evolve in a clocklike manner (Boore, 2006; Boore and Fuerstenberg, 2008). This approach is useful for resolving difficult branching points that occur in situations where a short period of shared evolutionary history is followed by a long period of divergence, causing a low signal to noise ratio (Boore and Fuerstenberg, 2008).

However, homoplastic gene orders have been reported more often than expected, assuming the statistical scenario described above. A well-known example is the mtDNA GO homoplasy in some birds (Mindell et al., 1998), although these orders differ in the position of the control region. Beyond this, several other (putative) homoplasy examples have been reported: *Locusta migratoria* (Orthoptera) and *Apis mellifera* (Hymenoptera) exhibit the same *trnD-trnK* arrangement (Flook et al., 1995), the GO of some ants (Hymenoptera: Formicidae) is identical to the one exhibited by a majority of the species of the Order Lepidoptera (Babbucci et al., 2014), and some isopod suborders exhibit local homoplastic rearrangements (Kilpert et al., 2012).

The flatworm (Platyhelminthes) subphylum Neodermata (obligatory parasites) is divided into three classes: Trematoda, Monogenea and Cestoda (Gibson et al., 2014). The GOs of Neodermata are generally considered to be conserved (Littlewood et al., 2006; Webster and Littlewood, 2012; Wey-Fabrizius et al., 2013). However, extensive GO rearrangements have been reported within the trematode genus *Schistosoma* (Digenea: Schistosomatidae) (Le et al., 2000, 2001; Littlewood et al., 2006; Sato et al., 2008; Wang et al., 2011; Webster and Littlewood, 2012), where a proportion of species exhibit a plesiomorphic GO, similar to cestodes and other trematodes, whereas other species possess strikingly derived GOs (Webster and Littlewood, 2012). Apart from this, recent investigations of neodermatan GOs exposed several other outliers with highly rearranged gene orders, all belonging to the class Monogenea. At the time when this study was conducted, the outliers comprised all three available mitogenomes belonging to the subclass Polyopisthocotylea (*Pseudochauhannea macrorchis*, *Polylabris halichoeres* and *Microcotyle sebastis*) (Park et al., 2007; Wey-Fabrizius et al., 2013) and several mitogenomes from the subclass Monopisthocotylea. In the meantime, three more Polyopisthocotylea mitogenomes (almost complete) were sequenced, and they exhibit only one or two tRNA transpositions in comparison to *M. sebastis* (Zhang et al., 2018b). Among the Monopisthocotylea, *Aglaiogyrodactylus forficulatus* (Gyrodactylidea: Gyrodactylidae) (Bachmann et al., 2016) exhibits a comprehensive rearrangement of both PCGs and tRNAs, whereas *Paratetraonchoides inermis* (Tetraonchidea: Tetraonchoididae) (Zhang et al., 2017b) and two species of Diplectanidae (Dactylogyridea) (Zhang et al., 2018a) exhibit extensively reshuffled tRNA genes.

Previous studies on the evolutionary history of GO changes within the Neodermata were hampered by the very small amount of available data (von Nickisch-Rosenegk et al., 2001; Littlewood et al., 2006; Park et al., 2007). For example, a previous attempt to infer ancestral GOs for the Cestoda and Trematoda was highly speculative due to the absence of monogenean mitogenomes (Littlewood et al., 2006). Similarly, GOs were proposed as reliable markers to distinguish the Monogenea from Cestoda and Trematoda, as the Polyopisthocotylea (Monogenea) exhibit a unique GO (Park et al., 2007). However, this was invalidated later when the first Monopisthocotylea mitogenomes were sequenced, which revealed that the GO of Monopisthocotylea is similar to that of Cestoda and Trematoda (Huysse et al., 2008; Plaisance et al., 2007). As the number of available mitogenomes has rapidly increased in recent years, we conducted an overview of the Neodermata GOs in our recent research (Zhang et al., 2017b). We observed that

the GOs of two species belonging to two different orders within the class Monogenea were identical: *Paragyrodactylus variegatus* (order Gyrodactylidea) and *Tetrancistrum nebulosi* (order Dactylogyridea). This GO (the common GO henceforth) was also observed in two orders in the class Cestoda: Diphylobothriidea and a proportion of the Cyclophyllidea species (Li et al., 2017). This is an exciting finding, because the common GO was shared between phylogenetically distant orders, and even classes. If we a priori reject the possibility that our current understanding of the phylogeny of Neodermata is completely erroneous (i.e., that the distantly related species exhibiting the common GO might actually form a monophyletic clade), there are two possible hypotheses for this phenomenon: (1) the common GO has arisen independently in these lineages, i.e. homoplasy (convergent evolution); (2) the common GO was retained from the common ancestor of these lineages, i.e. plesiomorphy (shared ancestry).

As proposed by Littlewood et al. (2006) as well, a GO shared between Monogenea and Digenea/Cestoda would allow us to infer the plesiomorphic (ancestral) GO for the stem group Neodermata. However, this common GO was found in only two representatives of the whole class Monogenea: *P. variegatus* and *T. nebulosi* (Ancyrocephalinae). To attempt to improve the resolution, we tried to sequence additional mitogenomes of species belonging to under-represented taxa. Due to limited access to suitable samples and time constraints, we managed to sequence only the mitogenome of *Euryhaliotrema johni* (Ancyrocephalinae). Following this, we conducted comparative analyses of GOs in the entire Neodermata clade, with the goal of inferring the evolutionary history of GOs in this group of parasitic flatworms.

2. Materials and methods

2.1. Specimen collection and identification

Euryhaliotrema johni was obtained from *Lutjanus argentimaculatus* (Forsskal, 1775; Lutjanidae, Perciformes) caught by fishermen in the Daya Bay, Guangdong Province, P.R. China (22°42'58"–22°42'56" N; 114°32'16"–114°32'25"E) on 10th July, 2017. Parasites were identified morphologically under a light microscope according to the traits described in Kritsky and Diggles (2014). Additionally, to confirm the taxonomic identity, the 28S rRNA gene was amplified using universal primers (Wu et al., 2005) (Supplementary Data S1). The obtained sequence shares 99% identity with the corresponding *E. johni* homologs available in GenBank (accession number **DQ157657**). The samples are permanently stored as vouchers in 100% ethanol in the Parasitology and Coevolution Laboratory (room number 511), Institute of Hydrobiology, Chinese Academy of Sciences, Wuhan, P.R. China (Accession No. **IHB20180730001**).

2.2. DNA extraction, amplification, sequencing and annotation

Amplification and annotation of the mitogenome of *E. johni* were conducted following the procedure described previously (Li et al., 2017, 2018; Zhang et al., 2017a,b, 2018a; Zou et al., 2017), so details are provided in Supplementary Data S1. Software programs used include Primer Premier 5 (Lalitha, 2000), BLAST (Altschul et al., 1990), DNASTar v7.1 (Burland, 2000), MITOS (Bernt et al., 2013), ARWEN (Laslett and Canback, 2008), and DOGMA (Wyman et al., 2004).

2.3. Dataset construction

First, all available neodermatan mitogenome sequences were downloaded from GenBank (last accessed 22nd July, 2018), and

all gene names made uniform with the help of in-house GUI-based software, PhyloSuite (Zhang, D., Gao, F., Li, W.X., Jakovlić, I., Zou, H., Zhang, J., Wang, G.T., 2018a. PhyloSuite: an integrated and scalable desktop platform for streamlined molecular sequence data management and evolutionary phylogenetics studies. bioRxiv, doi: <https://doi.org/10.1101/489088>). Second, the obtained sequences were filtered to remove duplicates and different isolates belonging to the same species, resulting in a set of 117 sequences: 49 cestodes, 23 monogeneans and 45 trematodes. Following this, due to limitations of software programs that we planned to use, namely TreeREX (Bernt et al., 2008) and CREx (Bernt et al., 2007), mitogenomes with duplicated genes and incomplete sequences were removed from the dataset, resulting in the final count of 104 sequences. Finally, some misannotated genes were reannotated. These procedures and datasets are detailed in [Supplementary Tables S1 and S2](#). The number of unique GOs was extrapolated from these neodermatan mitogenomes.

2.4. Phylogeny

Reconstruction of the evolutionary pathways among GOs requires a pre-existing phylogram, so we first conducted phylogenetic analyses using neodermatan mitogenomes. As different taxonomic groups were not uniformly represented among these neodermatan mitogenomes, we picked 64 representatives for the phylogenetic task: 1–3 species per genus, covering three classes, and 19 orders/superfamilies ([Supplementary Table S3](#)). This procedure mainly culled species from genera with numerous representatives such as *Echinococcus* (eight) and *Taenia* (10). We ensured that we did not remove any species possessing a unique GO. Two species of the order Tricladida, *Crenobia alpina* (Dana, 1766) (KP208776) and *Obama* sp. (NC_026978), were used as outgroups, thus adding up to 66 mitogenomes in total. Two datasets were used for phylogenetic analysis: amino acid alignment of 12 protein coding genes (PCGAA dataset, <https://doi.org/10.17632/f4gjb99n85.2>) and codon-based alignment of nucleotide sequences of 12 protein coding genes + secondary structure alignment of 22 tRNAs and two rRNAs (PCGRT dataset, <https://doi.org/10.17632/g6yz9gw76s.2>). Data processing was conducted using PhyloSuite, MAFFT software (Katoh and Standley, 2013) and Gblocks (Talavera and Castresana, 2007) following the procedure published previously (Li et al., 2017; Liu et al., 2017; Zhang et al., 2017a,b, 2018a; Zou et al., 2017), so details are provided in [Supplementary Data S1](#). Phylogenetic analyses were performed using two different algorithms: maximum likelihood (ML) and Bayesian inference (BI). Optimal partitioning strategies for both datasets were calculated using PartitionFinder2 (Lanfear et al., 2017) with greedy algorithm and AICc criterion, and used to conduct phylogenetic analyses. ML analyses were conducted using RAxML (Stamatakis, 2014) using a ML + rapid bootstrap (BS) algorithm with 1000 replicates. BI analyses were conducted using MrBayes 3.2.6 (Ronquist et al., 2012) with default settings, and 5×10^6 metropolis coupled Markov chain Monte Carlo (MCMC) generations. Stationarity was considered to be reached when the average standard deviation of split frequencies was below 0.01, the estimated sample size (ESS) value was above 200, and the potential scale reduction factor (PSRF) approached 1. Apart from data partitioning, two additional approaches were used: one to account for the data heterogeneity (site heterogeneous model CAT + GTR) and one for the data heterotachy (GHOST) (Crotty et al., 2019). The CAT + GTR model (for both datasets) was implemented in PhyloBayes MPI 1.5a (Lartillot et al., 2013), and the analysis (with two MCMC chains) was stopped when the conditions considered to indicate a good run (PhyloBayes manual) were reached: maxdiff < 0.1 and minimum effective size > 300. The heterotachy model (GTR + H4 for PCGRT, mtZOA + H4

for PCGAA) was implemented in IQ-TREE 1.65 (Nguyen et al., 2015) with 10,000 ultrafast bootstrapping (Minh et al., 2013).

2.5. GO analysis

As the number of unique GOs (duplicate GOs were removed) was far smaller than the number of species used for the phylogenetic analysis, we selected 32 representatives to display (neodermatan gene orders dataset, <https://doi.org/10.17632/9csp3ywwprh.2>), according to three criteria: (i) if a GO was only found in one order (or superfamily), we chose one representative from this group; (ii) if there were two or more unique GOs in one order (or superfamily), we chose one representative per GO in this group; (iii) if one GO was shared by two or more orders (or superfamilies), we chose one representative per order (or superfamily). The relationship between species and representatives is listed in [Supplementary Table S4](#). GOs were visualised and annotated by iTOL (Letunic and Bork, 2016) with the help of several dataset files generated by PhyloSuite, as described in our recent papers (Li et al., 2017; Zhang et al., 2017b). CREx was used to calculate pairwise similarity scores between GOs and determine their rearrangement pathways under the common interval measurement model. Using the topologies generated by four methodologies (MrBayes, RAxML, IQ-TREE and PhyloBayes) and two datasets (PCGAA and PCGRT), ancestral GO reconstructions were conducted using the TreeREX and MLGO programs. TreeREX software (tree rearrangement explorer) invokes the CREx algorithm based on common intervals, which can help infer parsimonious rearrangement scenarios given a phylogenetic hypothesis (Bernt et al., 2007). A brief explanation of the strategy for TreeREX is also described in Babbucci et al. (2014). The MLGO algorithm for reconstructing ancestral genomic orders is based on a probabilistic method called PMAG, which is supposed to be faster and more precise than previously used InferCARSPro (probabilistic method) and GRAPPA (parsimonious method) algorithms (Hu et al., 2013). A phylogenetic tree based on the GO dataset was reconstructed using MLGO, with 1000 bootstrap replicates (Lin et al., 2013).

2.6. Data accessibility

Datasets are available in Mendeley Data as follows.

Neodermatan gene orders: <https://doi.org/10.17632/9csp3ywwprh.2>;

PCGAA: <https://doi.org/10.17632/f4gjb99n85.2>;

PCGRT: <https://doi.org/10.17632/g6yz9gw76s.2>.

3. Results

3.1. Mitogenomic architecture of *E. johnei*

The complete mitogenome of *E. johnei* is 14,132 bp long (GenBank accession number MH700477), with 66% A + T content. All typical 36 flatworm mitochondrial genes are present, including 12 protein encoding genes (PCGs; *atp8* is absent), 22 tRNA genes, and two rRNA genes ([Supplementary Fig. S1](#)). An abbreviated stop codon (T-) was found in *cox3*, whereas the remaining PCGs use canonical stop codons TAA and TAG. The GO of *E. johnei* was identical to that of *T. nebulosi*. Therefore, both available (complete) mitogenomes belonging to the subfamily Ancyrocephalinae exhibit the common GO.

3.2. Phylogenies used for ancestral GO reconstruction and phylogenetic position of *E. johnei*

Topologies produced by two molecular datasets (nucleotides and amino acids) and different methodological approaches, site

heterogeneous (PCGRT_PB and PCGAA_PB), heterotachous (PCGRT_IQ and PCGAA_IQ), and data partitioning (PCGRT_ML, PCGAA_ML, PCGRT_BI and PCGAA_BI, [Supplementary Table S5](#)), are shown in [Supplementary Fig. S2](#). All eight analyses produced identical deep level topology, but unique shallow level topologies. The consensus deep topology is: Polyopisthocotylea, (Monopisthocotylea, (Cestoda, Trematoda)) ([Supplementary Fig. S2](#)). Inconsistency was mainly located in interordinal relationships within the subclass Monopisthocotylea, and classes Cestoda and Trematoda (also in inter-superfamily relationships in this class, [Supplementary Fig. S2](#)). We present all of these incompatible topologies in [Supplementary Fig. S3](#), and selected PCGRT_IQ topology is shown in [Fig. 1](#), as the GHOST model is able to account for rate variation across sites and lineages ([Crotty et al., 2019](#)). In detail: four different topologies were produced for the Monopisthocotylea: (1) topology1: (Tetraonchidea, Gyrodactylidea), (*Lepidotrema longipenis*, (Capsalidea, Dactylogyridea)); (2) topology2: Dactylogyridea, (Capsalidea, (*L. longipenis*, (Tetraonchidea, Gyrodactylidea))); (3) topology3 (*L. longipenis* clustered in the Dactylogyridea clade): (Tetraonchidea, Gyrodactylidea), (Capsalidea, Dactylogyridea); (4) topology4: (Capsalidea, Dactylogyridea), (*L. longipenis*, (Tetraonchidea, Gyrodactylidea)) (note that *L. longipenis* is a member of Dactylogyridea); two different topologies were found in Cestoda: (1) topology1: Caryophyllidea, ((Bothriocephalidea, Diphyllbothriidea), (Onchoproteocephalidea, Cyclophyllidea)); (2) topology2: Caryophyllidea, (Bothriocephalidea, (Diphyllbothriidea, (Onchoproteocephalidea, Cyclophyllidea))); four different topologies were also observed in the Trematoda: (1) topology1: Schistosomatoidea, (*Clinostomum complanatum*, (Pronocephaloidea, Paramphistomoidea), (Echinostomatoidea, (Gorgoderoidea,

(Opisthorchioidea, (Allocreadioidea, *Paragonimus ohirai*)))); (2) topology2: Schistosomatoidea, ((Pronocephaloidea, Paramphistomoidea), (Echinostomatoidea, (Gorgoderoidea, (Opisthorchioidea, (*P. ohirai*, Allocreadioidea))))); (3) topology3: Schistosomatoidea, (*C. complanatum*, (Gorgoderoidea, (Echinostomatoidea, ((Pronocephaloidea, Paramphistomoidea), (*P. ohirai*, (Allocreadioidea, Opisthorchioidea)))))); (4) topology4: Schistosomatoidea, (Gorgoderoidea, (Echinostomatoidea, ((Pronocephaloidea, Paramphistomoidea), (*P. ohirai*, (Allocreadioidea, Opisthorchioidea)))) (note that *P. ohirai* belongs to the Gorgoderoidea, and *C. complanatum* belongs to Schistosomatoidea) ([Supplementary Fig. S3](#)). Following a methodology used to resolve a similar problem encountered in insects previously ([Babbucci et al., 2014](#)), in order to test the effect of this topological instability on the ancestral GO reconstruction, we used all of the obtained topologies ([Supplementary Fig. S3](#)) to infer the most plausible evolutionary history of the neodermatan GO. None of the topologies produced for the three major groups (Monopisthocotylea, Trematoda and Cestoda) were in agreement with the topologies previously generated with denser sampling ([Boeger and Kritsky, 2001](#); [Olson et al., 2003](#); [Waeschenbach et al., 2012](#)). Therefore, we added three topologies produced by other studies to the ancestral GO reconstruction analysis: (1) topology5 of Monopisthocotylea (based on 66 homologous series of morphological characters ([Boeger and Kritsky, 2001](#))): Capsalidea, (Dactylogyridea, (Tetraonchidea, Gyrodactylidea)); (2) topology3 of Cestoda (based on combined mtDNA sequences and nuclear sequences ([Waeschenbach et al., 2012](#))): Caryophyllidea, (Diphyllbothriidea, (Bothriocephalidea, (Onchoproteocephalidea, Cyclophyllidea))); (3) topology5 of Trematoda (based on 18S rDNA and 28S rDNA ([Olson et al., 2003](#))): Schistosomatoidea, ((Prono-



Fig. 1. The evolution of gene orders (GOs) in the Neodermata. Nodes are coloured according to the output of TreeREx software: a green branch point represents a consistent node with the highest level of certainty, yellow represents a k-consistent (less reliable) node with an intermediate level of certainty, whereas red indicates a fallback node with the highest level of uncertainty. Orders (or superfamilies) are displayed on the right. The deduced neodermatan ancestral gene order is displayed along the top. Internal nodes which putatively retained the ancestral neodermatan gene order are labelled "common GO", where a reddish-purple label indicates that the same result was predicted by both TreeREx and MLGO softwares, a blue label indicates results predicted solely by the MLGO, and a green label indicates that result is a product of our own reasoning. The red branches denote the path from the common ancestor of Neodermata to species which retained the ancestral neodermatan gene order. (For interpretation of the references to colour in this figure legend, the reader is referred to the web version of this article.)

cephaloidea, Paramphistomoidea), (Echinostomatoidea, (Opisthorchioidea, (Gorgoderoidea, Allocreadioidea))).

The phylogenetic position of *E. johni* was also not stable: it either grouped with *Dactylogyrus lamellatus* (Dactylogyrinae subfamily), or with *T. nebulosi* (Ancyrocephalinae subfamily) (Supplementary Fig. S2). As *E. johni* belongs to the Ancyrocephalinae, this subfamily was resolved as paraphyletic in the former case.

3.3. GO of the subphylum Neodermata

We identified 22 unique GOs in the Neodermata, 13 of which were found among the 20 available monogenean mitogenomes (belonging to five orders, Supplementary Fig. S4; Table 1). Amongst these 13 unique GOs, six were remarkably rearranged, including those belonging to *P. inermis*, *A. forficulatus*, *L. longipenis* and all three polyopisthocotylids (*Pseudochauhannea macrorchis*, *Microcotyle sebastis* and *Polylabris halichoeres*), but the three polyopisthocotylid GOs were mutually similar (Fig. 1). The common interval analysis of GOs conducted using CREx produced low similarity scores between these species and other neodermatans (Table 1). The mitochondrial GO of Cestoda appears to be remarkably conserved (Fig. 1), with only four unique GOs among all 48 available mitogenomes belonging to five orders (Supplementary Fig. S4). We found six unique GOs among the Trematoda (36 available mitogenomes belonging to seven superfamilies, Supplementary Fig. S4), two of which are shared by different superfamilies (Fig. 1, Table 1). The first shared GO (named here tre1GO) is found in the superfamilies Schistosomatoidea, Echinostomatoidea and Opisthorchioidea, whereas the second shared GO (tre2GO) is found in Pronocephaloidea, Paramphistomoidea, Echinostomatoidea, and Gorgoderoidea.

3.4. Reconstruction of the ancestral GO for the subphylum Neodermata

Regardless of the topology used (eight new and three from other studies, see Section 3.2 and Supplementary Fig. S3), results of both MLGO and TreeREx analyses (two methods × 11 topologies, totalling 22 reconstructions) consistently indicated that the ‘common GO’ (as defined in the Introduction) represented the ancestral state for Cestoda (node 17), Monopisthocotylea (node 28), Cestoda + Trematoda (node 18), Cestoda + Trematoda + Monopisthocotylea (node 29), and Neodermata (node 30) (Fig. 1, Supplementary Fig. S3). Among the currently available data, we identified 32 species possessing the ‘common GO’ in two platyhelminth parasitic groups: Monogenea and Cestoda (Supplementary Fig. S4). In Monogenea, the ‘common GO’ was identified in: *P. variegatus* in the order Gyrodactylida, and two species in the order Dactylogyrida (*T. nebulosi* and *E. johni*). Additionally, *Cichlidogyrus* (Ancyrocephalidae/Ancyrocephalinae) species (Vanhove et al., 2018) probably also exhibit the ‘common GO’, but the mitogenome of *C. mbirizei* is incomplete, and the annotation of *C. halli* is unconfirmed. In Cestoda, 29 species exhibited the ‘common GO’: six in the Diphyllbothriidea order and 23 in the Cyclophyllida order (Supplementary Fig. S4).

3.5. The phylogeny of Neodermata inferred from GOs

We reconstructed a phylogeny of Neodermata using gene orders (MLGO algorithm). The four species possessing the ‘common GO’, three species possessing tre1GO and five species possessing tre2GO formed separate clades (Fig. 2, named ‘the common GO clade’, ‘tre1GO clade’ and ‘tre2GO clade’). Only a minor fragment of the topology was congruent with the topology inferred using sequence-based datasets (Fig. 2).

Table 1
Pairwise comparisons of mitochondrial gene orders among 22 neodermatan representatives. Numbers represent similarity scores between gene orders, where ‘1254’ signifies identical gene orders, and shading indicates different degrees of gene order similarity: light to dark = similar to dissimilar. Taxon names in the column heading are represented by acronyms.

	Sh	Os	Fg	Bg	Tr	Sm	So	Ks	Cv	Tn	Gn	Gk	Nm	Bh	Bs	DI	LI	PI	Af	Ms	Pm	Ph
<i>Schistosoma haematobium</i> NC_008074	1254	228	212	110	272	228	92	74	108	112	116	102	106	104	70	102	48	48	98	46	28	34
<i>Ogmocotyle sikae</i> OHX NC_027112	228	1254	1186	448	706	608	774	664	796	808	756	422	740	756	406	786	264	148	210	152	112	114
<i>Fasciola gigantica</i> NC_024025	212	1186	1254	408	658	564	822	712	840	850	796	424	796	796	414	832	304	148	224	166	114	120
<i>Brachycladium goliath</i> NC_029757	110	448	408	1254	236	224	466	364	448	456	426	266	414	426	206	442	186	112	176	102	90	86
<i>Trichobilharzia regenti</i> NC_009680	272	706	658	236	1254	1120	394	320	420	434	402	214	420	402	264	408	194	158	174	102	62	66
<i>Schistosoma mekongi</i> AF217449	228	608	564	224	1120	1254	372	282	372	384	354	190	372	354	236	362	178	190	156	88	60	64
<i>Senga ophioccephalina</i> NC_034715	92	774	822	466	394	372	1254	822	1056	1052	990	514	990	990	480	932	322	174	278	126	112	112
<i>Khawia sinensis</i> NC_034800	74	664	712	364	320	282	822	1254	834	836	782	382	782	782	400	724	316	158	230	118	112	108
<i>Cladoaenia vulturi</i> KU559932	108	796	840	448	420	372	1056	834	1254	1186	1120	574	1120	1120	546	1056	322	160	370	144	110	118
<i>Tetrancistrum nebulosi</i> NC_018031	112	808	850	456	434	384	1052	836	1186	1254	1186	638	1186	1186	580	1120	322	162	322	154	112	114
<i>Gyrodactylus nyanzae</i> MG970256	116	756	796	426	402	354	990	782	1120	1186	1254	688	1120	1120	552	1056	292	146	344	164	122	124
<i>Gyrodactylus kobayashii</i> NC_030050	102	422	424	266	214	190	514	382	574	638	688	1254	622	660	342	608	110	94	252	132	116	118
<i>Neobenedenia mellei</i> JQ038228	106	740	796	414	420	372	990	782	1120	1186	1120	622	1254	1120	546	1056	292	148	302	152	110	114
<i>Benedenia hoshinai</i> NC_014591	104	756	796	426	402	354	990	782	1120	1186	1120	660	1120	1254	610	1056	292	146	302	148	106	108
<i>Benedenia senoiata</i> NC_014291	70	406	414	206	264	236	480	400	546	580	552	342	546	610	1254	514	162	84	184	140	98	100
<i>Dactylogyrus lamellatus</i> KR871673	102	786	832	442	408	362	932	724	1056	1120	1056	608	1056	1056	1056	514	1254	306	322	136	112	112
<i>Lepidotrema longipenis</i> NC_039617	48	264	304	186	194	178	322	316	322	322	292	110	292	292	162	306	1254	182	146	82	78	80
<i>Paratetraochoidea inermis</i> KY856918	48	148	148	124	158	190	174	158	160	162	146	94	148	146	84	162	182	1254	108	52	50	50
<i>Agiatogyrodactylus forficulatus</i> KU679421	98	210	224	176	174	156	278	230	370	322	344	252	302	302	184	322	146	108	1254	68	64	68
<i>Microcotyle sebastis</i> NC_009055	46	152	166	102	102	88	126	118	144	154	164	132	152	148	140	136	82	52	68	1254	810	928
<i>Pseudochauhannea macrorchis</i> NC_016950	28	112	114	90	62	60	112	112	110	112	122	116	110	106	98	112	78	50	64	810	1254	762
<i>Polylabris halichoeres</i> NC_016057	34	114	120	86	66	64	112	108	118	114	124	118	114	108	100	112	80	50	68	928	762	1254

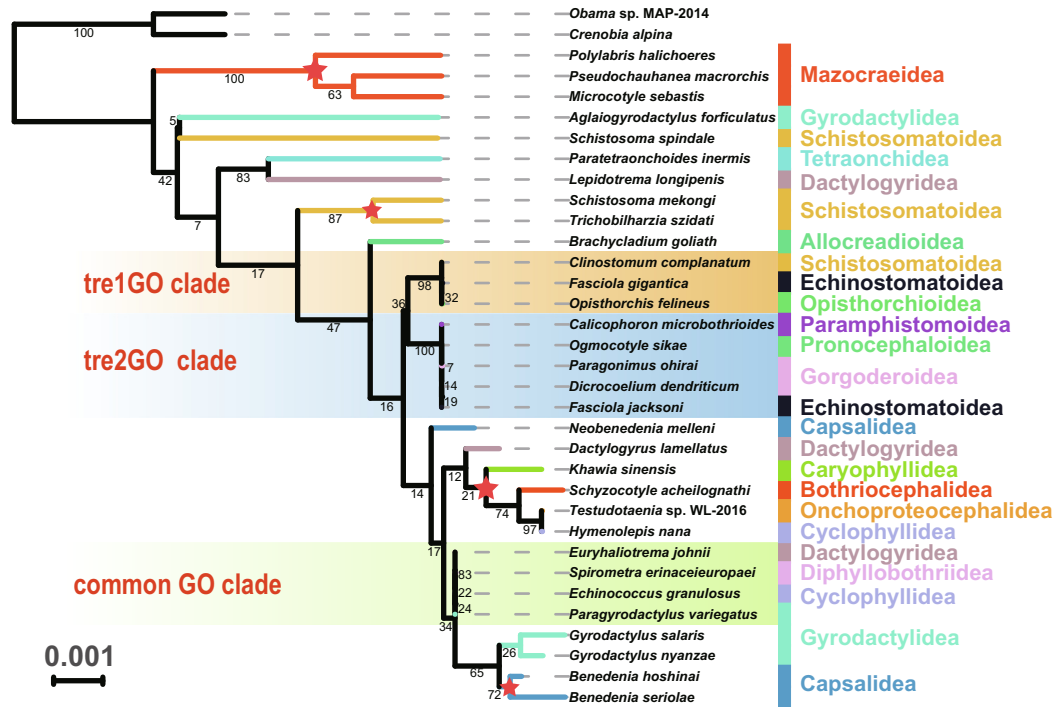


Fig. 2. Phylogenetic tree based on the gene order dataset. Taxonomic identity (orders or superfamilies) is displayed on the right. The numbers on branches denote bootstrap support values. Clades that exhibit similar topologies with Fig. 1 are marked with red stars on the nodes. See Section 3.3 for explanations of tre1GO, tre2GO and common GO.

4. Discussion

The chaotic (i.e., permeated by numerous deeply contradictory hypotheses) phylogeny of Neodermata was reflected in our phylogenetic reconstructions, where all eight analyses produced unique topologies. However, topological instability was limited to the lower level topology, whereas (sub)class level phylogeny was consistently supported by all inferred topologies: Polyopisthocotylea, (Monopisthocotylea, (Cestoda, Trematoda)) (Supplementary Fig. S2). Our results therefore reject the ‘Cercomeromorphae’ theory (Trematoda is a sister clade to Monogenea + Cestoda), supported by several early studies (Brooks, 1989; Littlewood et al., 1999a, 1999b; Littlewood and Olson, 2001; Zamparo et al., 2001), but later consistently rejected by mitochondrial phylogenomics studies (Park et al., 2007; Perkins et al., 2010), by a microRNA study (Fromm et al., 2013), by a multigene (312 genes) phylogenetic study (Hahn et al., 2014), and by a transcriptomic phylogenomics analysis (Egger et al., 2015). As Polyopisthocotylea and Monopisthocotylea subclasses belong to the class Monogenea, this topology rendered the Monogenea paraphyletic. Although paraphyletic Monogenea was also obtained in an early mitochondrial phylogenomics study with fewer monogenean representatives, in that topology the Cestoda + Trematoda clade formed a sister clade with Polyopisthocotylea (Perkins et al., 2010), instead of Monopisthocotylea, as in our results. The monophyly of Ancyrocephalinae was often debated in earlier studies (Kritsky and Boeger, 1989; Plaisance et al., 2005; Simkova et al., 2003, 2006; Vanhove et al., 2018), and our results also remain ambiguous (equally support and reject) about the monophyly/paraphyly of Ancyrocephalinae.

Given this context of an unresolved and unstable phylogeny of Neodermata, and as all (eight) of our methodological approaches produced different topologies, we were not sure which of these topologies is the ‘correct’ one, so we had to test whether and how the topological instability affects the reconstruction of GOs.

Furthermore, as these eight topologies differed from some previous phylogenetic hypotheses, we added three more topologies from previous studies (to complement our mitochondrial data, they are based on morphological and/or nuclear datasets, and denser samples; also see Section 3.2). All of the 22 ancestral GO reconstruction results (11 topologies × 2 methods) consistently resolved the common ancestor of all Neodermata (node 30), Cestoda (node 17), Monopisthocotylea (node 28), Cestoda + Trematoda (node 18), Cestoda + Trematoda + Monopisthocotylea (node 29) as possessing the common GO. Although the TreeREx reconstruction of node 30 was flagged as not fully reliable (yellow, Fig. 1, Supplementary Fig. S3), we hypothesise that the underlying reason is the absence of the common GO from all available Polyopisthocotylea mitogenomes, which is the earliest branch in the Neodermata phylogeny. Although we inferred that the common GO was retained throughout all of the common ancestors leading to the extant species possessing the common GO (‘the common GO scenario’ henceforth), this scenario is not fully supported by all of our ancestral reconstruction results (Fig. 1, Supplementary Fig. S3). For example, TreeREx predicted a derived GO (node 27 in the Fig. 1) in the path from the ancestral neodermatan to *P. variegatus*, comprising a rearrangement of the ‘common GO’ by a tandem-duplication-random-loss (TDRL) event (node 27), followed by a successive reversion (transposition events between successive nodes 26, 25 and *P. variegatus*) to the common GO (Supplementary Fig. S3, Topology1). While it is theoretically possible that the ancestral common GO underwent rearrangements in subsequent ancestral nodes and then again reverted to the ancestral condition (the common GO) in some of the species (branches highlighted in red in Fig. 1), we argue that this scenario is highly unlikely. The parsimony criterion (Fertin et al., 2009) implies that evolutionary scenarios requiring a smaller number of gene order rearrangements are more likely to reflect the actual course of events (Oxusoff et al., 2018). As a result, identical genome level characters (GO, specifically) are unlikely to be independently derived (homoplastic) and unlikely to revert to

an ancestral condition (GO irreversibility hypothesis) (Boore and Fuerstenberg, 2008). In agreement with this, the TreeREx reconstruction of node 27 was flagged as unreliable (printed in red) by the algorithm (Bernt et al., 2008), and MLGO predicted that node 27 retained the common GO (Supplementary Fig. S3, Topology1). Similarly, there are additional ancestral nodes leading to the contemporary ‘common GO’ species for which TreeREx and MLGO algorithms did not predict the ‘common GO’: nodes 13, 14, 24 and 25 in the MLGO reconstruction, and nodes 24–26 and 13–16 in the TreeREx reconstruction. Following the logic outlined above, we can reject these results as non-parsimonious, and accept the more parsimonious ‘common GO scenario’: the common GO was retained in all of the common ancestors leading up to present day species possessing the common GO. This also suggests that we can reject our first working hypothesis and conclude that the ‘common GO’ found in evolutionarily distant lineages is not a homoplasy. Instead, the entire lineage of common ancestors leading up to the species exhibiting the ‘common GO’ most likely retained the plesiomorphic ancestral GO of all Neodermata. Although topological instability affected the reconstruction of some internal nodes, it did not affect these two main findings: determining common GO as ancestral GO of five major taxonomic groups and the ‘common GO scenario’. Specifically, although the status of Ancyrocephalidae/Ancyrocephalinae is debatable, and the phylogenetic position of *E. johni* unstable, alternative phylogenetic hypotheses would not affect these two conclusions. The only hypothetical finding that would affect the reliability of the ‘common GO scenario’ would be a discovery of another apparently homoplastic GO shared by several evolutionarily distant species. As such a phenomenon has not yet been identified, we can accept the ‘common GO scenario’ as the most parsimonious.

Topological congruence between the GO tree (Fig. 2) and molecular sequence-based trees (Fig. 1, Supplementary Fig. S2) was observed predominantly in taxa with highly rearranged GOs shared within lineages: (i) due to their highly variable GOs (although similar to each other) in comparison to other neodermatans, the three polyopisthocotyliids (*P. macrorchis*, *M. sebastis* and *P. halichoeres*) formed the most basal branch within the Neodermata; (ii) *S. mekongi* and *T. szidati* formed a sister group (probably due to peculiar *cox3-trnE-trnH-cytb* and *nad2-trnA-trnD-nad1* arrangements); (iii) the affinity of *B. seriolae* and *B. hoshinai* (supported by the specific *trnF-trnQ-trnM* arrangement). However, the GO topology is mostly incongruent with the sequence-based topologies, and there is evidence for artefactual homoplastic clustering of conserved GOs (for example, common GO clade, tre1GO clade and tre2GO clade in Fig. 2). This is strong evidence that GOs are prone to producing phylogenetic artefacts, and should be used with utmost caution for phylogenetic reconstruction in this group of animals. Although highly rearranged GOs did produce some phylogenetic congruence with molecular data, we suspect that they may be prone to producing disproportionately long branches (Zou et al., 2017), which may result in long branch attraction artefacts. Therefore, we propose that derived GOs may be useful only for resolving specific taxonomic uncertainties; for example, the strikingly rearranged GOs exhibited by some schistosomes were exploited as an excellent marker to distinguish between two different clades of schistosomes (Littlewood et al., 2006; Webster and Littlewood, 2012).

4.1. Tracing the evolutionary scenarios amongst the GOs of Monogenea

Unique GOs in the class Monogenea accounted for more than half of the total number of unique GOs identified in the Neodermata. As some of the monogenean GOs were conserved (in comparison to the ‘common GO’), while some were highly rearranged (Table 1), this corroborates that the evolution of GOs in the class

Monogenea is highly discontinuous (Zhang et al., 2017b, 2018a). The common GO found in two phylogenetically distant lineages (represented by *P. variegatus* and *E. johni*, Fig. 1) of the class Monogenea allowed us to infer the GO of the ancestral lineages connecting these two species. Following the ‘common GO scenario’ outlined in the previous section, all internal nodes of the Monopisthocotylea subclass phylogram probably possessed the ancestral GO of Neodermata, with the exception of nodes 19 and 20 (Fig. 1). The Plesiomorphic GO of the order Capsalidea (node 20) was identical to that of Neodermata, whereas the GO of *Benedenia hoshinai* was resolved as the ancestral GO for node 19 in all reconstructions (Supplementary Fig. S3). Most of the GO transformational pathways from common ancestors to their descendants required only one transposition event; examples are node 24 to *G. nyanzae* (transposal of *trnF*), node 21 to *D. lamellatus* (transposal of *trnL2*), node 20 to *N. melleni* (transposal of *trnG*), node 20 to node 19 (transposal of *trnQ*), and node 19 to *B. seriolae* (transposal of *trnT*) (Fig. 3). It is noteworthy that the TDRL event in the pathway from node 25 to *G. salaris* indirectly corroborates our plesiomorphic GO reconstruction (ancestral GO of *G. salaris* is the common GO), because a reversal of this rearrangement would require two transpositions (Fig. 4). This conforms to the hypothesis that TDRL events generate directional information, as reversing the rearrangement would require more than a single operation, so TDRL is considered to be an “irreversible” change (Perseke et al., 2008; Babbucci et al., 2014). This is also a more likely scenario according to the parsimony criterion (Fertin et al., 2009). However, the three hypervariable GOs (*P. inermis*, *A. forficulatus* and *L. longipenis*) underwent a series of complicated rearrangements since these species split from their most recent common ancestors (Fig. 3). In detail: the transformational pathway from node 27 to *P. inermis* required three coupled moves (one transposition and two TDRLs) and one TDRL operation; the pathway from node 26 to *A. forficulatus* required three transpositions and one TDRL operation; the pathway from node 23 to *L. longipenis* required two transpositions, two coupled transpositions and one TDRL event (Fig. 3). A GO different from the common GO was resolved as ancestral for the Polyopisthocotylea by both algorithms, which implies that a common ancestor of this group may have undergone a GO rearrangement. More specifically, TreeREx and MLGO reconstructions actually predicted two GOs that differed only in the position of *trnL1* (Supplementary Fig. S3, all 11 topologies). However, as the reconstruction was flagged as unreliable (red) in TreeREx, and as we had a limited number of samples for Polyopisthocotylea at our disposal, we cannot conclude this with confidence. This hypothesis would be invalidated if future studies managed to identify a Polyopisthocotylea species possessing the common GO.

The evolutionary scenario of monogenean GO rearrangements confirms the hypothesis that genome level characters evolve in a saltatory (non-clocklike) manner (Boore and Fuerstenberg, 2008). It is also in agreement with the hypothesis that once a long period of stasis in the GO evolution is interrupted, this often results in an exponential acceleration of subsequent rearrangements (Zou et al., 2017), as observed in the three hypervariable GOs here, in nematodes (Zou et al., 2017), snails (Wang et al., 2017), insects (Xiong et al., 2013) and vertebrates (Mueller and Boore, 2005).

4.2. Tracing the evolutionary scenarios amongst the GOs of Cestoda

As we discussed in a recent paper (Li et al., 2017), all of the observed rearrangements in the class Cestoda took place in the rearrangement hot spot comprising four tRNA genes: *trnY*, *trnL1*, *trnL2* and *trnS2* (see also Fig. 1). According to our results here, the GO currently exhibited by some members of the Cyclophyllidea (but see also Cyclophyllidea group 2 in Li et al. (2017)) and Diphyllbothriidea is identical to the common GO, and thus plesiomor-



Fig. 3. Rearrangement scenarios from ancestors to their descendants. Rearrangement events are indicated in curly brackets, wherein square brackets indicate coupled rearrangement events. The gene blocks involved in rearrangement events are coloured yellow. TDRL, tandem-duplication-random-loss event; T, transposition event. (For interpretation of the references to colour in this figure legend, the reader is referred to the web version of this article.)

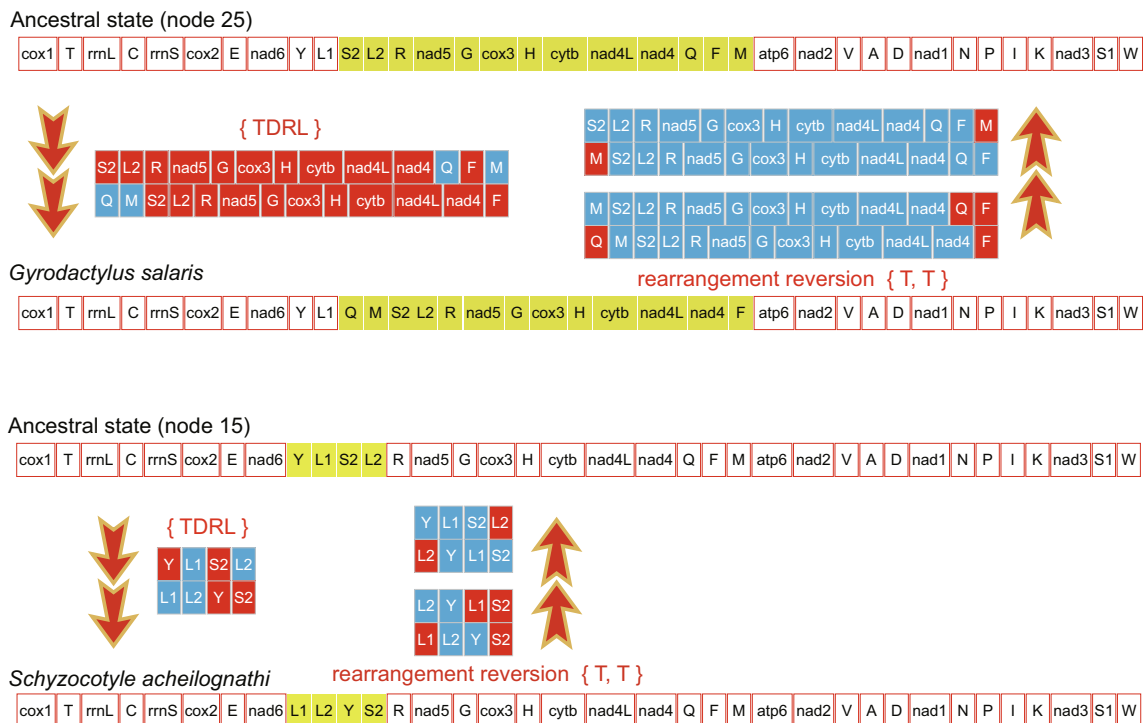


Fig. 4. Transformational pathways between *Gyrodactylus salaris*, *Schyzocotyle acheilognathi* and their ancestors. The transformational pathway from ancestors to species is shown on the left, whereas the pathway from species to ancestors is displayed on the right. TDRL, tandem-duplication-random-loss event; T, transposition event.

phic for nodes 13–17 according to the ‘common GO scenario’ (Fig. 1). Consequently, the transformational pathway from the common GO to the first unique GO (represented by *Khawia sinensis*; Fig. 1) required a transposition of the *trnL1-trnS2-trnL2* gene block. The pathway from the common GO to the second unique GO (*Testudotaenia* sp. and *Hymenolepis nana*) required a transposition of *trnS2*. Finally, the pathway from the common GO to the third unique GO (*Schyzocotyle acheilognathi*) required one TDRL event (Fig. 3). Most importantly, as discussed in the previous section and by Li et al. (2017), the TDRL event in the last case implies the order of events, because reversing this TDRL event would require two transpositions (Fig. 4). In other words, the common GO is plesiomorphic, whereas the third unique GO is derived, which is an important finding that confirms our hypothesis regarding the antiquity of the common GO.

4.3. Tracing the evolutionary scenarios amongst the GOs of Trematoda

Previous GO studies within the Trematoda were mainly concentrated on the radically altered GO observed in the genus *Schistosoma*, as the remaining (available) trematodes have relatively conserved GOs, exhibiting only minor tRNA rearrangements (Fig. 1). Similar to the limitations discussed above, tre1GO and tre2GO complicate the ancestral GO reconstruction in Trematoda. In order to infer which of the two GOs is ancestral (plesiomorphic), we have to rely on the topology to infer the ‘earliest branch’ in the evolutionary history. As both require only one transposition to be rearranged into/from the common GO (with *trnE* transposed to the *nad5-cox3* junction and near *trnG*: *trnE-trnG* in tre1GO versus *trnG-trnE* in tre2GO; Fig. 1), this renders the comparison with the common GO useless for resolving this issue. In our topologies (Supplementary Fig. S2), as well as the topologies inferred in other studies (Olson et al., 2003; Le et al., 2016), the only species exhibiting the tre1GO in Schistosomatoidea (*C. complanatum*) either clustered with the superfamily Schistosomatoidea (order Diplostomida) (see PCGRT_PB and PCGAA_PB in the Supplementary Fig. S2, and previous phylogenetic studies based on 18S rDNA and 28S rDNA (Olson et al., 2003)) or formed a sister group with the remainder of Trematoda (order Plagiorchiida), thus implying that it branches off early in the evolutionary history from the base of the Trematoda. We therefore cautiously hypothesise that tre1GO predates (is ancestral to) tre2GO. There is additional evidence to support this: (i) two *Diplostomum* spp. (Schistosomatoidea superfamily; not included in this study due to being incomplete), which clustered with *C. complanatum* (Le et al., 2016), also exhibit the *trnE-trnG* (tre1GO) arrangement; (ii) tre1GO was shared both by the Orders Diplostomida and Plagiorchiida, whereas tre2GO was only observed in the Plagiorchiida; (iii) CREx analysis showed that tre1GO had a higher similarity score (850) than tre2GO (808) to the ancestral GO of neodermatans (represented by *E. johnei* in Table 1); (iv) a majority of MLGO reconstructions (apart from the analyses of the Monopisthocotylea topology 5, and Trematoda topologies 2 and 4) and all TreeREx reconstructions indicated that tre1GO is the ancestral condition for all topologies (Supplementary Fig. S3). On the basis of these observations, the results of TreeREx, and following the logic of ‘common GO scenario’, we cautiously propose that nodes 5 and 7–11 represent the ancestral GO state of Trematoda (node 12, tre1GO) (Fig. 1, Supplementary Fig. S3). The tre2GO was the ancestral state of the stable (Supplementary Fig. S2) suborder Pronocephalata (node 4; Orders Pronocephaloidea and Paramphistomoidea). The transformational pathway from the ancestral GO in the node 10 to that of the node 4 required a simple *trnE-trnG* to *trnG-trnE* rearrangement (Fig. 3). The same rearrangement was required in an additional two places: node 5 to Echinostomatoidea (*Fasciola jacksoni*), and node 8 to Gorgoderoidea (*D. dendriticum*). We will not further discuss the GO

evolution of Gorgoderoidea (*P. ohirai*), Allocreadioidea and Schistosomatoidea orders (nodes 2, 3 and 6) as these reconstructions were highly uncertain, but results can be viewed in Supplementary Fig. S3.

4.4. Dataset limitations and future directions

As mentioned in the introduction, we suspected before beginning this study that more data might be needed in order to assess the two working hypotheses. Unfortunately, due to limited accessibility of the taxa of interest and time constraints, we managed to obtain only a sample of an ancyrocephalid species, *E. johnei*, for this study. In order to reconstruct the ancestral GO for Trematoda with certainty, we would need a stable topology, for which we would require much better taxon sampling, with a focus on representatives of the subclass Aspidogastrea, which is considered to be a relatively old group in the Trematoda (Rohde et al., 2001; Olson et al., 2003), so we hypothesise that its GO might be pivotal for this purpose. Additionally, due to their phylogenetic importance, sequencing of additional mitogenomes belonging to the following lineages might help shed light on the evolutionary history of mitogenomic architecture in the Neodermata: polystomatoinean monogeneans (Monogenea: Polystomatoinea), additional ancyrocephalids (Monogenea: Monopisthocotylea: Dactylogyridea), species belonging to the subclass Cestodaria (Cestoda) and species belonging to the suborder Bucephalata (Trematoda: Digenea: Plagiorchiida). Apart from sequencing additional mitogenomes, future studies should also attempt to conduct a molecular dating analysis to approximately time the origin of pivotal taxa.

The analyses presented here shed new light on the evolution of mitogenomic architecture in the subphylum Neodermata. Our results show that the common GO is shared by two classes, four orders and 32 species is the ancestral (plesiomorphic) GO state for the Neodermata and most other major taxonomic groups: Monopisthocotylea, Monopisthocotylea + Cestoda + Trematoda, Cestoda + Trematoda, and Cestoda. This conclusion is further supported by the GO irreversibility hypothesis and two “irreversible” TDRL events inferred in the Monogenea and Cestoda classes. Expanding on this, we proposed that all ancestral nodes leading up to the present day species exhibiting the ‘common GO’ were most likely to possess the plesiomorphic GO of Neodermata. This allowed us to propose transformational pathways from each common ancestor to its descendants amongst the Monogenea and Cestoda classes. We also proposed a putative ancestral GO for the class Trematoda. The sister clade relationship of Polyopisthocotylea and the remaining neodermatans was corroborated by the GO analysis, but it should be corroborated by nuclear data as well. Highly derived GOs, found in the Monogenea and Trematoda clades, reflect the saltatory nature of the evolution of mitochondrial architecture. Although highly derived GOs may have some potential for taxon identification, whereas identical GOs found in distant lineages may be valuable resources to determine the ancestral GO, GOs are prone to producing artefactual relationships in phylogenetic analyses, and should be used with utmost caution for phylogenetic reconstruction in Neodermata. Our analysis was hampered by poor sampling of many neodermatan taxa, so sequencing of further mitogenomes is urged in order to generate a sufficient amount of data to infer the evolutionary pathways leading to the observed diversity of GOs with confidence, especially the hypervariable but underrepresented Monogenea and poorly resolved Trematoda classes.

Acknowledgements

This work was supported by the National Natural Science Foundation of China (grant numbers 31872604, 31572658); the Ear-

marked Fund for China Agriculture Research System (grant number CARS-45-15); and the Major Scientific and Technological Innovation Project of Hubei Province, P.R. China (grant number 2015ABA045). We would also like to thank the editor and the two anonymous reviewers for the time they invested in reviewing our manuscript.

Appendix A. Supplementary data

Supplementary data to this article can be found online at <https://doi.org/10.1016/j.ijpara.2019.05.010>.

References

- Altschul, S.F., Gish, W., Miller, W., Myers, E.W., Lipman, D.J., 1990. Basic local alignment search tool. *J. Mol. Biol.* 215, 403–410.
- Babbucci, M., Basso, A., Scupola, A., Patarnello, T., Negrisol, E., 2014. Is it an ant or a butterfly? Convergent evolution in the mitochondrial gene order of Hymenoptera and Lepidoptera. *Genome Biol. Evol.* 6, 3326–3343.
- Bachmann, L., Fromm, B., de Azambuja, L.P., Boeger, W.A., 2016. The mitochondrial genome of the egg-laying flatworm *Aglaiogyrodactylus forficulatus* (Platyhelminthes: Monogeneoidea). *Parasit. Vectors* 9, 285.
- Bernt, M., Merkle, D., Ramsch, K., Fritsch, G., Perseke, M., Bernhard, D., Schlegel, M., Stadler, P.F., Middendorf, M., 2007. CREx: inferring genomic rearrangements based on common intervals. *Bioinformatics* 23, 2957–2958.
- Bernt, M., Merkle, D., Middendorf, M., 2008. An algorithm for inferring mitogenome rearrangements in a phylogenetic tree. In: Nelson, C.E., Viallette, S. (Eds.), *Comparative Genomics, International Workshop, RECOMB-CG 2008, Proceedings of Lecture Notes in Bioinformatics*. Springer, pp. 143–157.
- Bernt, M., Donath, A., Juhling, F., Externbrink, F., Florentz, C., Fritsch, G., Putz, J., Middendorf, M., Stadler, P.F., 2013. MITOS: improved de novo metazoan mitochondrial genome annotation. *Mol. Phylogenet. Evol.* 69, 313–319.
- Boeger, W.A., Kritsky, D.C., 2001. Phylogenetic relationships of the Monogeneoidea. In: Littlewood, D.T.J., Bray, R.A. (Eds.), *Interrelationships of the Platyhelminthes*. Taylor & Francis, London, pp. 92–102.
- Boore, J., 2006. The use of genome-level characters for phylogenetic reconstruction. *Trends Ecol. Evol.* 21, 439–446.
- Boore, J.L., Brown, W.M., 1998. Big trees from little genomes: mitochondrial gene order as a phylogenetic tool. *Curr. Opin. Genet. Dev.* 8, 668–674.
- Boore, J.L., Fuerstenberg, S.I., 2008. Beyond linear sequence comparisons: the use of genome-level characters for phylogenetic reconstruction. *Philos. Trans. R. Soc. Lond. B. Biol. Sci.* 363, 1445–1451.
- Brooks, D.R., 1989. The phylogeny of the Cercomeria (Platyhelminthes: Rhabdocoela) and general evolutionary principles. *J. Parasitol.* 606–616.
- Burland, T.G., 2000. DNASTAR's Lasergene sequence analysis software. *Methods Mol. Biol.* 132, 71–91.
- Crotty, S.M., Minh, B.Q., Bean, N.G., Holland, B.R., Tuke, J., Jermiin, L.S., von Haeseler, A., 2019. GHOST: Recovering historical signal from heterotachously-evolved sequence alignments. *Syst. Biol.* <https://doi.org/10.1093/sysbio/syz051>.
- Dobzhansky, T., Sturtevant, A.H., 1938. Inversions in the chromosomes of *Drosophila Pseudoobscura*. *Genetics* 23, 28–64.
- Egger, B., Lapraz, F., Tomiczek, B., Muller, S., Dessimoz, C., Girstmair, J., Skunca, N., Rawlinson, K.A., Cameron, C.B., Beli, E., Todaro, M.A., Gammoudi, M., Norena, C., Telford, M.J., 2015. A transcriptomic-phylogenomic analysis of the evolutionary relationships of flatworms. *Curr. Biol.* 25, 1347–1353.
- Fertin, G., Labarre, A., Rusu, I., Viallette, S., Tannier, E., 2009. Combinatorics of Genome Rearrangements. MIT Press, Cambridge, Massachusetts.
- Floork, P., Rowell, H., Gellissen, G., 1995. Homoplastic rearrangements of insect mitochondrial tRNA genes. *Naturwissenschaften* 82, 336–337.
- Fromm, B., Worren, M.M., Hahn, C., Hovig, E., Bachmann, L., 2013. Substantial loss of conserved and gain of novel MicroRNA families in flatworms. *Mol. Biol. Evol.* 30, 2619–2628.
- Gibson, D.I., Bray, R.A., Hunt, D., Georgiev, B.B., Scholz, T., Harris, P.D., Bakke, T.A., Pojmanska, T., Niewiadomska, K., Kostadinova, A., Tkach, V., Bain, O., Durette-Desset, M.C., Gibbons, L., Moravec, F., Petter, A., Dimitrova, Z.M., Buchmann, K., Valtonen, E.T., de Jong, Y., 2014. Fauna europaea: helminths (animal parasitic). *Biodivers. Data J.* 2, e1060.
- Hahn, C., Fromm, B., Bachmann, L., 2014. Comparative genomics of flatworms (platyhelminthes) reveals shared genomic features of ecto- and endoparasitic neodermata. *Genome Biol. Evol.* 6, 1105–1117.
- Hu, F., Zhou, L., Tang, J., 2013. Reconstructing ancestral genomic orders using binary encoding and probabilistic models. *Bioinformatics Res. Appl. Lecture Notes Comput. Sci.* 7875, 17–27.
- Huysse, T., Buchmann, K., Littlewood, D.T., 2008. The mitochondrial genome of *Gyrodactylus derjavinoi* (Platyhelminthes: Monogenea) – a mitogenomic approach for *Gyrodactylus* species and strain identification. *Gene* 417, 27–34.
- Katoh, K., Standley, D.M., 2013. MAFFT multiple sequence alignment software version 7: improvements in performance and usability. *Mol. Biol. Evol.* 30, 772–780.
- Kilpert, F., Held, C., Podsiadlowski, L., 2012. Multiple rearrangements in mitochondrial genomes of Isopoda and phylogenetic implications. *Mol. Phylogenet. Evol.* 64, 106–117.
- Kritsky, D.C., Boeger, W.A., 1989. The phylogenetic status of the Ancyrocephalidae Bychowksy, 1937 (Monogenea: Dactylogyroidea). *J. Parasitol.* 207–211.
- Kritsky, D.C., Diggles, B.K., 2014. Dactylogyrids (Monogeneoidea: Polyonchoinea) parasitising the gills of snappers (Perciformes: Lutjanidae): species of *Euryhaliotrema* Kritsky & Boeger, 2002 from the golden snapper *Lutjanus johnii* (Bloch) off northern Australia, with a redescription of *Euryhaliotrema johnii* (Tripathi, 1959) and descriptions of two new species. *Syst. Parasitol.* 87, 73–82.
- Lalitha, S., 2000. Primer Premier 5. Biot. Soft. Int. Rep. 1, 270–272.
- Lanfear, R., Frandsen, P.B., Wright, A.M., Senfeld, T., Calcott, B., 2017. PartitionFinder 2: new methods for selecting partitioned models of evolution for molecular and morphological phylogenetic analyses. *Mol. Biol. Evol.* 34, 772–773.
- Lartillot, N., Rodrigue, N., Stubbs, D., Richer, J., 2013. PhyloBayes MPI: phylogenetic reconstruction with infinite mixtures of profiles in a parallel environment. *Syst. Biol.* 62, 611–615.
- Laslett, D., Canback, B., 2008. ARWEN: a program to detect tRNA genes in metazoan mitochondrial nucleotide sequences. *Bioinformatics* 24, 172–175.
- Le, T.H., Blair, D., Agatsuma, T., Humair, P.F., Campbell, N.J.H., Iwagami, M., Littlewood, D.T.J., Peacock, B., Johnston, D.A., Bartley, J., 2000. Phylogenies inferred from mitochondrial gene orders – a cautionary tale from the parasitic flatworms. *Mol. Biol. Evol.* 17, 1123–1125.
- Le, T.H., Humair, P.-F., Blair, D., Agatsuma, T., Littlewood, D.T., McManus, D.P., 2001. Mitochondrial gene content, arrangement and composition compared in African and Asian schistosomes. *Mol. Biochem. Parasitol.* 117, 61–71.
- Le, T.H., Nguyen, N.T.B., Nguyen, K.T., Doan, H.T.T., Dung, D.T., Blair, D., 2016. A complete mitochondrial genome from *Echinochasmus japonicus* supports the elevation of Echinochasmidae Ochner, 1910 to family rank (Trematoda: Platyhelminthes). *Infect. Genet. Evol.* 45, 369–377.
- Letunic, I., Bork, P., 2016. Interactive tree of life (iTOL) v3: an online tool for the display and annotation of phylogenetic and other trees. *Nucleic Acids Res.* 44, W242–245.
- Li, W.X., Zhang, D., Boyce, K., Xi, B.W., Zou, H., Wu, S.G., Li, M., Wang, G.T., 2017. The complete mitochondrial DNA of three monozoic tapeworms in the Caryophyllidea: a mitogenomic perspective on the phylogeny of eucestodes. *Parasit. Vectors* 10, 314.
- Li, W.X., Fu, P.P., Zhang, D., Boyce, K., Xi, B.W., Zou, H., Li, M., Wu, S.G., Wang, G.T., 2018. Comparative mitogenomics supports synonymy of the genera *Ligula* and *Digramma* (Cestoda: Diphylobothriidae). *Parasit. Vectors* 11, 324.
- Lin, Y., Hu, F., Tang, J., Moret, B.M.E., 2013. Maximum likelihood phylogenetic reconstruction from high-resolution whole-genome data and a tree of 68 eukaryotes. *Pac. Symp. Biocomput.* 123, 285–296.
- Littlewood, D.T., Lockyer, A.E., Webster, B.L., Johnston, D.A., Le, T.H., 2006. The complete mitochondrial genomes of *Schistosoma haematobium* and *Schistosoma spindale* and the evolutionary history of mitochondrial genome changes among parasitic flatworms. *Mol. Phylogenet. Evol.* 39, 452–467.
- Littlewood, D.T.J., Olson, P.D., 2001. Small subunit rDNA and the Platyhelminthes: signal, noise, conflict and compromise. In: Littlewood, D.T.J., Bray, R.A. (Eds.), *Interrelationships of the Platyhelminthes*. Taylor & Francis, London, pp. 262–278.
- Littlewood, D., Rohde, K., Bray, R., Herniou, E., 1999a. Phylogeny of the Platyhelminthes and the evolution of parasitism. *Biol. J. Linn. Soc.* 68, 257–287.
- Littlewood, D., Rohde, K., Clough, K., 1999b. The interrelationships of all major groups of Platyhelminthes: phylogenetic evidence from morphology and molecules. *Biol. J. Linn. Soc.* 66, 75–114.
- Liu, F.-F., Li, Y.-P., Jakovlic, I., Yuan, X.-Q., 2017. Tandem duplication of two tRNA genes in the mitochondrial genome of *Tagiades vajuna* (Lepidoptera: Hesperidae). *Eur. J. Entomol.* 114, 407–415.
- Mindell, D.P., Sorenson, M.D., Dimcheff, D.E., 1998. Multiple independent origins of mitochondrial gene order in birds. *Proc. Natl. Acad. Sci. U S A* 95, 10693–10697.
- Minh, B.Q., Nguyen, M.A., von Haeseler, A., 2013. Ultrafast approximation for phylogenetic bootstrap. *Mol. Biol. Evol.* 30, 1188–1195.
- Mueller, R.L., Boore, J.L., 2005. Molecular mechanisms of extensive mitochondrial gene rearrangement in plethodontid salamanders. *Mol. Biol. Evol.* 22, 2104–2112.
- Nguyen, L.T., Schmidt, H.A., von Haeseler, A., Minh, B.Q., 2015. IQ-TREE: a fast and effective stochastic algorithm for estimating maximum-likelihood phylogenies. *Mol. Biol. Evol.* 32, 268–274.
- Olson, P.D., Cribb, T.H., Tkach, V.V., Bray, R.A., Littlewood, D.T.J., 2003. Phylogeny and classification of the Digenea (Platyhelminthes: Trematoda). *Int. J. Parasitol.* 33, 733–755.
- Oxusoff, L., Prea, P., Perez, Y., 2018. A complete logical approach to resolve the evolution and dynamics of mitochondrial genome in bilaterians. *PLoS One* 13, e0194334.
- Park, J.K., Kim, K.H., Kang, S., Kim, W., Eom, K.S., Littlewood, D.T., 2007. A common origin of complex life cycles in parasitic flatworms: evidence from the complete mitochondrial genome of *Microcotyle sebastis* (Monogenea: Platyhelminthes). *BMC Evol. Biol.* 7, 11.
- Perkins, E.M., Donnellan, S.C., Bertozzi, T., Whittington, I.D., 2010. Closing the mitochondrial circle on paraphyly of the Monogenea (Platyhelminthes) infers evolution in the diet of parasitic flatworms. *Int. J. Parasitol.* 40, 1237–1245.
- Perseke, M., Fritsch, G., Ramsch, K., Bernt, M., Merkle, D., Middendorf, M., Bernhard, D., Stadler, P.F., Schlegel, M., 2008. Evolution of mitochondrial gene orders in echinoderms. *Mol. Phylogenet. Evol.* 47, 855–864.
- Plaisance, L., Littlewood, D.T.J., Olson, P.D., Morand, S., 2005. Molecular phylogeny of gill monogeneans (Platyhelminthes, Monogenea, Dactylogyridae) and colonization of Indo-West Pacific butterflyfish hosts (Perciformes, Chaetodontidae). *Zool. Scr.* 34, 425–436.

- Plaisance, L., Huysse, T., Littlewood, D.T., Bakke, T.A., Bachmann, L., 2007. The complete mitochondrial DNA sequence of the monogenean *Gyrodactylus thymalli* (Platyhelminthes: Monogenea), a parasite of grayling (*Thymallus thymallus*). *Mol. Biochem. Parasitol.* 154, 190–194.
- Rohde, K., Littlewood, D., Bray, R., 2001. The Aspidogastrea, an archaic group of Platyhelminthes. In: Littlewood, D.T.J., Bray, R.A. (Eds.), *Interrelationships of the Platyhelminthes*. Taylor & Francis, London, pp. 159–167.
- Ronquist, F., Teslenko, M., van der Mark, P., Ayres, D.L., Darling, A., Höhna, S., Larget, B., Liu, L., Suchard, M.A., Huelsenbeck, J.P., 2012. MrBayes 3.2: efficient Bayesian phylogenetic inference and model choice across a large model space. *Syst. Biol.* 61, 539–542.
- Sato, Y., Le, T.H., Hiraike, R., Yukawa, M., Sakai, T., Rajapakse, R.P., Agatsuma, T., 2008. Mitochondrial DNA sequence and gene order of the Sri Lankan *Schistosoma nasale* is affiliated to the African/Indian group. *Parasitol. Int.* 57, 460–464.
- Simkova, A., Plaisance, L., Matejusova, I., Morand, S., Verneau, O., 2003. Phylogenetic relationships of the Dactylogyridae Bychowsky, 1933 (Monogenea: Dactylogyridae): the need for the systematic revision of the Ancyrocephalinae Bychowsky, 1937. *Syst. Parasitol.* 54, 1–11.
- Simkova, A., Matejusova, I., Cunningham, C.O., 2006. A molecular phylogeny of the Dactylogyridae sensu Kritsky & Boeger (1989) (Monogenea) based on the D1–D3 domains of large subunit rDNA. *Parasitology* 133, 43–53.
- Stamatakis, A., 2014. RAxML version 8: a tool for phylogenetic analysis and post-analysis of large phylogenies. *Bioinformatics* 30, 1312–1313.
- Talavera, G., Castresana, J., 2007. Improvement of phylogenies after removing divergent and ambiguously aligned blocks from protein sequence alignments. *Syst. Biol.* 56, 564–577.
- Vanhove, M.P.M., Briscoe, A.G., Jorissen, M.W.P., Littlewood, D.T.J., Huysse, T., 2018. The first next-generation sequencing approach to the mitochondrial phylogeny of African monogenean parasites (Platyhelminthes: Gyrodactylidae and Dactylogyridae). *BMC Genomics* 19, 520.
- von Nickisch-Roseneck, M., Brown, W.M., Boore, J.L., 2001. Complete sequence of the mitochondrial genome of the tapeworm *Hymenolepis diminuta*: gene arrangements indicate that platyhelminths are eutrochozoans. *Mol. Biol. Evol.* 18, 721–730.
- Waeschenbach, A., Webster, B.L., Littlewood, D.T., 2012. Adding resolution to ordinal level relationships of tapeworms (Platyhelminthes: Cestoda) with large fragments of mtDNA. *Mol. Phylogenet. Evol.* 63, 834–847.
- Wang, Y., Wang, C.R., Zhao, G.H., Gao, J.F., Li, M.W., Zhu, X.Q., 2011. The complete mitochondrial genome of *Orientobilharzia turkestanicum* supports its affinity with African *Schistosoma* spp. *Infect. Genet. Evol.* 11, 1964–1970.
- Wang, J.G., Zhang, D., Jakovlic, I., Wang, W.M., 2017. Sequencing of the complete mitochondrial genomes of eight freshwater snail species exposes pervasive paraphyly within the Viviparidae family (Caenogastropoda). *PLoS One* 12, e0181699.
- Webster, B.L., Littlewood, D.T.J., 2012. Mitochondrial gene order change in *Schistosoma* (Platyhelminthes: Digenea: Schistosomatidae). *Int. J. Parasitol.* 42, 313–321.
- Wey-Fabrizius, A.R., Podsiadlowski, L., Herlyn, H., Hankeln, T., 2013. Platyzoan mitochondrial genomes. *Mol. Phylogenet. Evol.* 69, 365–375.
- Wu, X.Y., Li, A.X., Zhu, X.Q., Xie, M.Q., 2005. Description of *Pseudorhabdosynochus seabassi* sp. n. (Monogenea: Diplectanidae) from Lates calcarifer and revision of the phylogenetic position of *Diplectanum grouperi* (Monogenea: Diplectanidae) based on rDNA sequence data. *Folia Parasitol.* 52, 231.
- Wyman, S.K., Jansen, R.K., Boore, J.L., 2004. Automatic annotation of organellar genomes with DOGMA. *Bioinformatics* 20, 3252–3255.
- Xiong, H., Barker, S.C., Burger, T.D., Raoult, D., Shao, R., 2013. Heteroplasmy in the mitochondrial genomes of human lice and ticks revealed by high throughput sequencing. *PLoS One* 8, e73329.
- Zamparo, D., Brooks, D.R., Hoberg, E.P., McLennan, D.A., 2001. Phylogenetic analysis of the Rhabdozoa (Platyhelminthes) with emphasis on the Neodermata and relatives. *Zool. Scr.* 30, 59–77.
- Zhang, D., Zou, H., Wu, S.G., Li, M., Jakovlic, I., Zhang, J., Chen, R., Wang, G.T., Li, W.X., 2017a. Sequencing, characterization and phylogenomics of the complete mitochondrial genome of *Dactylogyryrus lamellatus* (Monogenea: Dactylogyridae). *J. Helminthol.* 1–12.
- Zhang, D., Zou, H., Wu, S.G., Li, M., Jakovlic, I., Zhang, J., Chen, R., Wang, G.T., Li, W.X., 2017b. Sequencing of the complete mitochondrial genome of a fish-parasitic flatworm *Paratetraonchoides inermis* (Platyhelminthes: Monogenea): tRNA gene arrangement reshuffling and implications for phylogeny. *Parasit. Vectors* 10, 462.
- Zhang, D., Li, W.X., Zou, H., Wu, S.G., Li, M., Jakovlic, I., Zhang, J., Chen, R., Wang, G.T., 2018a. Mitochondrial genomes of two diplectanids (Platyhelminthes: Monogenea) expose paraphyly of the order Dactylogyridae and extensive tRNA gene rearrangements. *Parasit. Vectors* 11, 601.
- Zhang, D., Zou, H., Wu, S.G., Li, M., Jakovlic, I., Zhang, J., Chen, R., Li, W.X., Wang, G.T., 2018b. Three new Diplozoidae mitogenomes expose unusual compositional biases within the Monogenea class: implications for phylogenetic studies. *BMC Evol. Biol.* 18, 133.
- Zou, H., Jakovlic, I., Chen, R., Zhang, D., Zhang, J., Li, W.X., Wang, G.T., 2017. The complete mitochondrial genome of parasitic nematode *Camallanus cotti*: extreme discontinuity in the rate of mitogenomic architecture evolution within the Chromadorea class. *BMC Genomics* 18, 840.